

# Graph Encoder Ensemble for Simultaneous Vertex Embedding and Community Detection

Cencheng Shen, Youngser Park, Carey E. Priebe

**Abstract**—In this paper we propose a novel and computationally efficient method to simultaneously achieve vertex embedding, community detection, and community size determination. By utilizing a normalized one-hot graph encoder and a new rank-based cluster size measure, the proposed graph encoder ensemble algorithm achieves excellent numerical performance throughout a variety of simulations and real data experiments.

**Index Terms**—Graph Embedding, Vertex Clustering, L2 Normalization



## 1 INTRODUCTION

GRAPH data consists of a collection of vertices and edges representing the pairwise relationship. Given  $n$  vertices and  $s$  edges, a graph (or network) can be represented by an  $n \times n$  adjacency matrix  $\mathbf{A}$  where  $\mathbf{A}(i, j)$  is the edge weight between the  $i$ th vertex and  $j$ th vertex. In practice, it is often stored by an  $s \times 3$  edgelist  $\mathbf{E}$ , where the first two columns store the vertex indices of each edge and the last column is the edge weight.

Community detection [1], [2], [3], [4] is a fundamental problem for graph data. Often, the vertices can be naturally separated into several communities, where within-community vertices are more connected than between-community vertices. This problem is also called vertex clustering or graph partition, and many algorithms have been proposed on this end.

For example, embedding-based methods like adjacency or Laplacian spectral clustering are provably consistent under popular random graph models [5], [6], as well as likelihood-based techniques [4], [7] — however, they are typically slow and not scalable to large graphs. On the other hand, modularity-based methods like Louvain and Leiden are much faster and thus more popular in practice [8], [9] — however, there is relatively little theoretical investigation, and the output only has the community labels and no vertex embedding. Moreover, determining the community size is an important question on its own, but has mostly been ad-hoc or simply assumed known.

In this paper we design a graph encoder ensemble to simultaneously achieve graph embedding, community detection, and community-size determination. The ensemble algorithm utilizes a normalized one-hot graph encoder [10], ensemble learning [11], [12], k-means clustering [13], [14],

and a novel rank-based cluster size measure called minimal rank index to determine the best ensemble and the best community size. The proposed algorithm has a linear running time, is scalable to big graphs, and exhibits excellent numerical performance throughout our experiments. The code is made available on Github<sup>1</sup>.

## 2 GRAPH ENCODER ENSEMBLE

To better present the main algorithm, we introduce several auxiliary functions as follows: given an  $s \times 3$  edgelist  $\mathbf{E}$  with  $n$  vertices and a label vector  $\mathbf{Y} \in \mathbb{R}^n$  of  $k$  communities, we denote the one-hot graph encoder embedding as

$$\mathbf{Z} = \text{one-hot-emb}(\mathbf{E}, \mathbf{Y}),$$

where  $\mathbf{Z} \in \mathbb{R}^{n \times k}$  provides a  $k$ -dimensional representation for each vertex (see [10] for more details). Then the  $L_2$  normalization step is denoted as  $\mathbf{Z} = \text{normalize}(\mathbf{Z})$ , which normalizes each vertex representation to unit norm (see Section 2.2 for details). Moreover, given any embedding  $\mathbf{Z}$  and a label vector  $\mathbf{Y}$ , we denote the minimal rank index as  $\text{MRI}(\mathbf{Z}, \mathbf{Y}) \in [0, 1]$ , which measures the clustering quality and the smaller the better (details in Section 2.3). We also denote the k-means clustering as  $\text{k-means}(\mathbf{Z}, K)$ , and the adjusted rand index as  $\text{ARI}(\mathbf{Y}, \mathbf{Y}_2)$  between two label vectors of the same size. The ARI is a popular matching metric lies in  $(-\infty, 1]$ , with larger positive number implying better matchedness and 1 means perfect match [15].

In the following, we first present the main algorithm. The major innovations in the proposed algorithm, i.e.,  $L_2$  normalization, the minimal rank index, and ensemble embedding, are further explained in the remaining subsections.

### 2.1 Methodology

The method is detailed in Algorithm 1 and visualized in Figure 1. It is applicable to any binary or weighted graph, directed or undirected graph with or without self-loop. For the parameter choice, throughout this paper we set the number of random replicates  $r = 10$ , the number of

- Cencheng Shen is with the Department of Applied Economics and Statistics, University of Delaware. E-mail: shenc@udel.edu
- Carey E. Priebe and Youngser Park are with the Department of Applied Mathematics and Statistics (AMS), the Center for Imaging Science (CIS), and the Mathematical Institute for Data Science (MINDS), Johns Hopkins University. E-mail: cep@jhu.edu, youngser@jhu.edu

This work was supported in part by the National Science Foundation HDR TRIPODS 1934979, the National Science Foundation DMS-2113099, and by funding from Microsoft Research.

1. <https://github.com/cshen6/GraphEmd>

maximum iteration  $m = 20$ , and the clustering range shall be determined by the experiment under-consideration.

By design, the proposed algorithm achieves simultaneous vertex embedding, community detection, and cluster size determination. Note that the unsupervised graph encoder embedding in [10] can be viewed as a special case of the graph encoder ensemble at  $|R| = 1$  (the clustering range is a singleton) and  $r = 1$ .

---

### Algorithm 1 Graph Encoder Ensemble

---

**Require:** An edgelist  $\mathbf{E}$ , a range of potential cluster size  $R$ , number of random replicates  $r$ , and number of maximum iteration  $m$ .

**Ensure:** The graph embedding  $\mathbf{Z} \in \mathbb{R}^{n \times \hat{K}}$  for all vertices, the estimated number of clusters  $\hat{K}$ , the cluster indices  $\mathbf{Y} \in \mathbb{R}^n$ , and the minimal rank index  $ind \in [0, 1]$ .

**function** GRAPH-ENCODER-ENSEMBLE( $\mathbf{E}, R, r, m$ )

$ind = 1$ ;  $\triangleright$  initialize the index to pick best cluster size

**for**  $k \in R$  **do**

$ind_2 = 1$ ;  $\triangleright$  initialize the index to pick best

random replicate

**for**  $i = 1, \dots, r$  **do**

$\hat{\mathbf{Y}}_k = \text{rand}(k, n)$ ;  $\triangleright$  randomly initialize a label vector of length  $n$  in  $[k]$

**for**  $j = 1, \dots, m$  **do**

$\hat{\mathbf{Z}}_k = \text{one-hot-emb}(\mathbf{E}, \hat{\mathbf{Y}}_k)$ ;

$\hat{\mathbf{Z}}_k = \text{normalize}(\hat{\mathbf{Z}}_k)$ ;

$\hat{\mathbf{Y}}_k = \text{k-means}(\hat{\mathbf{Z}}_k, k)$ ;

**if**  $\text{ARI}(\hat{\mathbf{Y}}_k, \hat{\mathbf{Y}}_k') = 1$  **then break**;

**else**  $\hat{\mathbf{Y}}_k = \hat{\mathbf{Y}}_k'$ ;

**end if**

**end for**

$\hat{\mathbf{Z}}_k = \text{one-hot-emb}(\mathbf{E}, \hat{\mathbf{Y}}_k)$ ;

$\hat{\mathbf{Z}}_k = \text{normalize}(\hat{\mathbf{Z}}_k)$ ;

$ind_3 = \text{MRI}([\hat{\mathbf{Z}}_k, \hat{\mathbf{Y}}_k])$ ;

**if**  $ind_3 < ind_2$  **then**

$\hat{\mathbf{Z}} = \hat{\mathbf{Z}}_k$ ;  $\hat{\mathbf{Y}} = \hat{\mathbf{Y}}_k$ ;  $ind_2 = ind_3$ ;

**end if**

**end for**

**if**  $ind_2 \leq ind$  **then**

$\mathbf{Z} = \hat{\mathbf{Z}}$ ;  $\mathbf{Y} = \hat{\mathbf{Y}}$ ;  $\hat{K} = k$ ;  $ind = ind_2$ ;

**end if**

**end for**

**end function**

---

## 2.2 Why Normalization

The normalization step  $\text{normalize}()$  scales each vertex embedding to unit-norm in Algorithm 1, i.e., for each  $i$ , do

$$\mathbf{Z}(i, :) = \mathbf{Z}(i, :) / \|\mathbf{Z}(i, :)\|_2.$$

Figure 2 illustrates the difference between un-normalized and normalized embedding for a sparse and two-community random graph model. The normalized embedding is on a unit-circle, extracts the connectivity information and omits the vertex degree, thus better for clustering when the community information is solely determined by vertex connectivity (which translates to the block probability in the stochastic block model). Alternatively, using the normalized

embedding + k-means clustering is equivalent to using un-normalized embedding + angle / cosine / spherical k-means clustering.

The distinction here closely resembles the two-truth phenomenon between graph adjacency and graph Laplacian [16], i.e., the Laplacian spectral embedding (LSE) can be viewed as a degree-normalized version of adjacency spectral embedding (ASE), and typically performs better on sparse graphs. See Section 3.2 and Table 1 for more numerical evaluations on the normalization effect.

## 2.3 The Minimal Rank Index

To measure the clustering quality, we tailored a new rank-based measure called the minimal rank index (MRI). It is a key metric in Algorithm 1 to compare multiple embeddings from different initializations and different community sizes.

Let  $\mathbf{Y}_i$  denote the cluster index of vertex  $i$ ,  $d(\cdot, \cdot)$  denotes the Euclidean distance, and  $\mu_k$  denote the mean of  $k$ th cluster, i.e.,  $\mu_k = \sum_{i=1, \dots, n, \mathbf{Y}_i=k} \mathbf{Z}_i$ . The minimal rank index is computed as

$$\text{MRI} = \sum_{i=1, \dots, n} I\{\arg \min_{k=1, \dots, K} d(\mathbf{Z}_i, \mu_k) \neq \mathbf{Y}_i\} / n \in [0, 1]. \quad (1)$$

Namely, it measures how often the vertex embedding is not closest to its cluster mean. A smaller value suggests better clustering quality, and MRI equals 0 means every vertex is closest to its cluster mean. In the context of k-means clustering, MRI is non-zero when k-means does not converge.

Comparing to common cluster size measures like Silhouette Score, Davies Bouldin index, Variance Ratio Criterion, Gap criterion [17], [18], MRI is rank-based while others are based on actual distances, i.e., a ratio of within-cluster distance and between-cluster distance. If MRI is replaced by any of the other criterion in Algorithm 1, the cluster size choice will be biased towards the smallest possible. This is because of the unique incremental-dimension nature of graph encoder embedding: the embedding dimension of Algorithm 1 equals  $k$ , which is the community size. This makes the within-cluster distance smaller for smaller  $k$ , so any cluster size measure based on actual distances is biased towards smallest  $k$ . On the other hand, MRI is rank-based thus not susceptible to this issue, making it robust against varying dimensions. Section 3.4 and Figure 3 demonstrate this phenomenon via simulations.

## 2.4 Ensemble Embedding and Cluster Size Determination

By using a set of different models, ensemble learning is known to improve the learning performance and reduce the variance. This is employed in Algorithm 1 as follows: for each  $k$  in the cluster range, we compute a set of vertex embedding and community labels based on random label initialization, then choose the best one with the smallest MRI. If there are multiple models with the smallest MRI, we take the average embedding.

Next, among all possible cluster choice  $k$ , we also choose the best embedding with smallest MRI. In case of multiple

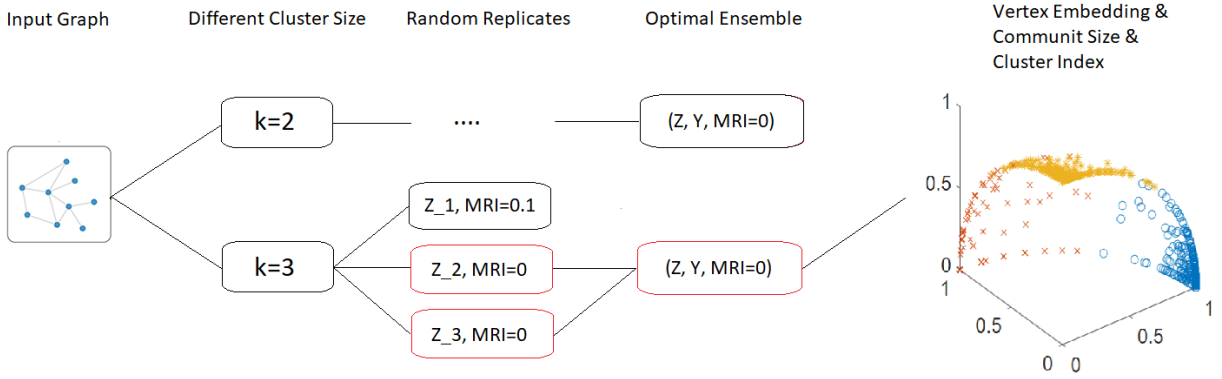


Fig. 1. Illustrate the graph encoder ensemble algorithm by a simple example.

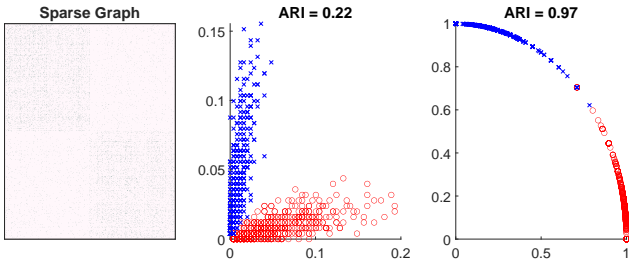


Fig. 2. The Normalization Effect: the left panel shows the adjacency heatmap of a simulated sparse graph using simulator 1 in Section 3.1; the center panel is the resulting embedding without the normalization step; and the right panel is the resulting embedding with normalization. The blue and red dots represent the true community of each vertex. The normalization clearly helps k-means clustering, which yields significantly better ARI vs ground-truth community labels.

embedding with the smallest MRI, we use the embedding with the largest  $k$ . For example, suppose the MRI is 0, 0, 0, 0.1, 0.2 for  $K = 2, 3, 4, 5, 6$ , then graph encoder ensemble shall choose  $\hat{K} = 4$ .

In the context of Algorithm 1, the ensemble embedding successfully mitigates potential bad initialization and significantly reduces the estimation variance. Section 3.3 and Table 2 demonstrate its numerical advantage.

### 2.5 Computational Complexity Analysis

Algorithm 1 consists of one-hot graph encoder embedding, k-means clustering, MRI computation, and ensembles. Denote  $n$  as the number of vertices and  $s$  as the number of edges. At any fixed  $k$ , the one-hot graph encoder embedding takes  $O(nk + s)$ , k-means takes  $O(nk)$ , the MRI computation takes  $O(nk)$ . Therefore, Algorithm 1 runs in  $O(rm(n \max(R) + s))$ , i.e., linear with respect to the number of vertices and edges. Similarly, the storage requirement is just  $O(n \max(R) + s)$ . When testing on simulated graphs using default parameters and  $\max(R) = 10$ , the graph encoder ensemble takes  $< 3$  minutes to process 1 million edges and  $< 20$  minutes for 10 million edges, which is extremely fast and scalable.

For even larger graph, the loops in Algorithm 1 can be easily parallelized for more time reduction: The embedding and MRI can be computed in parallel at each replicate and

each cluster size, before computing the optimal MRI and outputting the final results. This reduces the running time to  $O(n \max(R) + s)$ , same as the storage requirement.

## 3 EXPERIMENTS

In this section we carry out comprehensive numerical experiments to showcase the advantage of the graph encoder ensemble, as well as the individual benefits of normalization, ensemble, and MRI. The benchmarks are the same algorithm without normalization; without ensemble; MRI replaced; as well as the adjacency / Laplacian spectral embedding. We use ARI to measure the matchedness between the ground-truth labels and the estimated communities.

### 3.1 Simulation Set-up

The stochastic block model (SBM) is arguably the most fundamental community-based random graph model [19], [20]. Each vertex  $i$  is associated with a class label  $Y_i \in \{1, \dots, K\}$ . The class label may be fixed a-priori, or generated by a categorical distribution with prior probability  $\{\pi_k \in (0, 1) \text{ with } \sum_{k=1}^K \pi_k = 1\}$ . Then a block probability matrix  $\mathbf{B} = [\mathbf{B}(k, l)] \in [0, 1]^{K \times K}$  specifies the edge probability between a vertex from class  $k$  and a vertex from class  $l$ : for any  $i < j$ ,

$$\begin{aligned} \mathbf{A}(i, j) &\stackrel{i.i.d.}{\sim} \text{Bernoulli}(\mathbf{B}(Y_i, Y_j)), \\ \mathbf{A}(i, i) &= 0, \quad \mathbf{A}(j, i) = \mathbf{A}(i, j). \end{aligned}$$

The degree-corrected stochastic block model (DC-SBM) [3] is a generalization of SBM to better model the sparsity of real graphs. Everything else being the same as SBM, each vertex  $i$  has an additional degree parameter  $\theta_i$ , and the adjacency matrix is generated by

$$\mathbf{A}(i, j) \sim \text{Bernoulli}(\theta_i \theta_j \mathbf{B}(Y_i, Y_j)).$$

For our simulations, we consider the following four DC-SBM models with increasing community size. In all four models, we use the same degree distribution  $\theta_i \stackrel{i.i.d.}{\sim} \text{Beta}(1, 4)$ .

Simulation 1:  $n = 3000$ ,  $K = 2$ ,  $Y_i = \{1, 2\}$  equally likely, and the block probability matrix is

$$\mathbf{B} = \begin{bmatrix} 0.5, 0.1 \\ 0.1, 0.5 \end{bmatrix}.$$

Simulation 2:  $n = 5000$ ,  $K = 3$ ,  $Y_i = \{1, 2, 3\}$  with prior probability  $[0.2, 0.3, 0.5]$ , and the block probability matrix is

$$\mathbf{B} = \begin{bmatrix} 0.9, 0.1, 0.1 \\ 0.1, 0.5, 0.1 \\ 0.1, 0.1, 0.2 \end{bmatrix}.$$

Simulation 3:  $n = 3000$ ,  $K = 4$ ,  $Y_i = \{1, 2, 3, 4\}$  with prior probability  $[0.2, 0.2, 0.3, 0.3]$ , and the block probability matrix is

$$\mathbf{B} = \begin{bmatrix} 0.9, 0.1, 0.1, 0.1 \\ 0.1, 0.7, 0.1, 0.1 \\ 0.1, 0.1, 0.5, 0.1 \\ 0.1, 0.1, 0.1, 0.3 \end{bmatrix}.$$

Simulation 4:  $n = 3000$ ,  $K = 5$ ,  $Y_i$  with equally likely prior probability, and the block probability matrix satisfies:  $\mathbf{B}(i, i) = 0.2$  and  $\mathbf{B}(i, j) = 0.1$  for all  $i = 1, \dots, 5$  and  $j \neq i$ .

### 3.2 Normalization Comparison

Table 1 clearly shows that the clustering ARI using normalized algorithm far exceeds the ARI using the un-normalized algorithm. To exclude other factors in this comparison, we simply use  $r = 1$  and assume known cluster size. As expected, the phenomenon also happens between ASE and LSE, as LSE is also a normalized version of ASE.

	ARI			
	GEE	GEE (no norm)	ASE	LSE
Simulation 1	<b>0.91</b>	0.10	0.23	<b>0.91</b>
Simulation 2	0.71	0.17	0.27	<b>0.75</b>
Simulation 3	<b>0.73</b>	0.08	0.12	0.65
Simulation 4	<b>0.78</b>	0.06	0.17	<b>0.78</b>

TABLE 1

Evaluate the normalization effect in Graph Encoder Ensemble.

### 3.3 Ensemble Comparison

In this simulation we continue to assume known cluster size, carry out 100 Monte-Carlo replicates, and report ARI between the ensemble embedding ( $r = 10$ ) and the no-ensemble embedding ( $r = 1$ ). Table 2 shows that the ensemble algorithm clearly outperforms the no-ensemble version: the mean ARI is improved and variance is significantly reduced.

Empirically, the default choice of  $r = 10$  worked sufficiently well throughout our experiments, and we do not observe any significant gain for larger  $r$ . Moreover, if the graph size is sufficiently large and the community structure is sufficiently separable, using a smaller  $r$  or even  $r = 1$  suffices, which is the case for simulation 1 in Table 2.

	Average ARI + std	
	GEE	GEE ( $r = 1$ )
Simulation 1	0.91 ± 0.01	0.91 ± 0.01
Simulation 2	0.81 ± 0.01	0.71 ± 0.16
Simulation 3	0.79 ± 0.02	0.72 ± 0.09
Simulation 4	0.89 ± 0.01	0.79 ± 0.12

TABLE 2

Evaluate the ensemble advantage in Graph Encoder Ensemble. After 100 Monte-Carlo replicates, the mean and standard deviation of ARI are reported.

### 3.4 Cluster Size Estimation

Here we investigate how well the algorithm estimates the community size. Instead of using the ground-truth size, we let  $R = 2, 3, \dots, 10$  and report the results in Figure 3. The left panel shows the accuracy of community size estimation as sample size increases: as  $n$  increases, graph encoder ensemble has better and better estimation accuracy, which eventually reaches 1. As MRI is key to the size determination, the center panel shows the average MRI for simulation 4 (true  $K = 5$ ): the ensemble algorithm is able to accurately estimate the truth, because the largest community size that minimizes the MRI is indeed 5. The right panel shows the ensemble algorithm that replaces MRI by the Silhouette Score (the larger the better): the Silhouette Score biases towards the smallest cluster size and forces the algorithm to choose two communities instead. This phenomenon is consistent throughout all our simulations and experiments, as well as other size measures like DB-index or variance ratio.

## 4 REAL DATA

In this section we consider the following real data from network repository<sup>2</sup> [21] and Stanford network data<sup>3</sup>: Cora Citations (2708 vertices, 5429 edges, 7 classes), Industry Partnerships (219 vertices, 630 edges, 3 classes), EU Email Network [22] (1005 vertices, 25571 edges, 42 classes), and Political Blogs [23] (1490 vertices, 33433 edges, 2 classes).

The benchmarks are LSE assuming true  $K$ , graph encoder ensemble assuming true  $K$ , graph encoder ensemble estimating  $K$  via MRI, and graph encoder ensemble estimating  $K$  via Silhouette Score. The resulting ARI score is reported in Table 3: the ensemble algorithm using known  $K$  is the best performer; and in case of unknown  $K$ , though it does not pick the ground-truth community size, the performance is still relatively good.

However, even if the real data comes with ground-truth, it is often debate-able whether the ground-truth truly reflects the nature of the connectivity. Take the political blog data as an example: the blogs were manually separated into the Republican and Democratic blogs, but naturally the swing voters matter the most. Interestingly, when not assuming the true  $K = 2$ , the graph encoder ensemble does pick three communities from the data. Figure 4 visualizes the difference: the left panel visualizes the encoder embedding using ground-truth label at  $K = 2$ , while the

2. <https://networkrepository.com/index.php>

3. <https://snap.stanford.edu/>



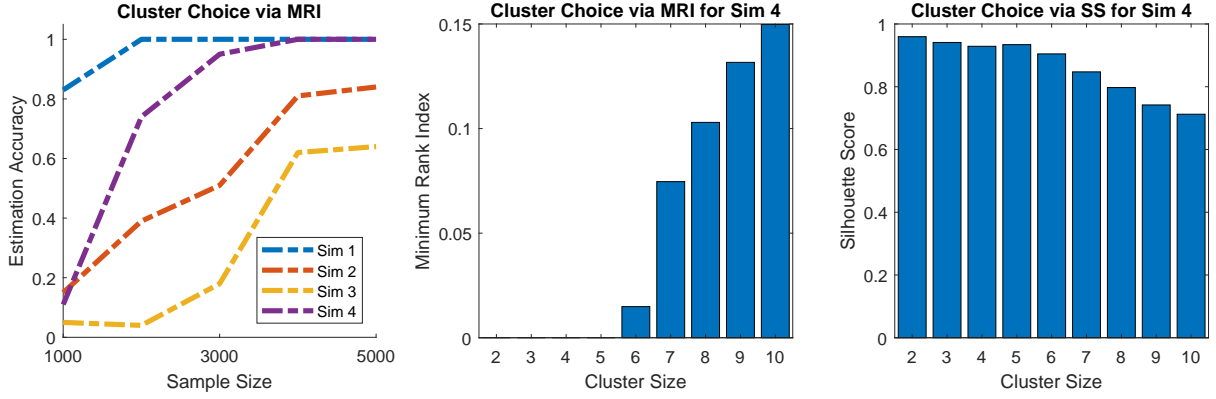


Fig. 3. Demonstrate the cluster size estimation in graph encoder ensemble. For each simulation and each graph size, we independently generate 100 graphs, and run the ensemble algorithm to estimate the community size. The left panel shows the estimation accuracy as graph size grows, i.e., how often the algorithm chooses the correct community size. As graph size increases, the estimation accuracy gradually increases to 1 for all simulations. The center panel shows the average MRI at  $n = 5000$  for simulation 4, where  $\hat{K} = 5$  is the estimated size and also the ground-truth size. The right panel shows the average Silhouette Score, where  $\hat{K}_{SS} = 2$  would be the choice.

	True $K$	GEE	LSE	R	GEE using $\hat{K}$	GEE using $\hat{K}_{SS}$
Cora Citations	7	0.11	0.08	2-20	0.07(3)	0.03(2)
Emails	42	0.48	0.23	10-50	0.39(14)	0.28(10)
Industry	3	0.13	0.13	2-10	0.08(5)	0.07(2)
Political blogs	2	0.80	0.80	2-10	0.69(3)	0.80(2)

TABLE 3  
Real Data Experiments.

right panel visualizes the ensemble embedding estimating 3 communities. Surprisingly, the encoder ensemble did an excellent job in identifying neutral / swing blogs, providing valuable insights not available from the ground-truth labels.

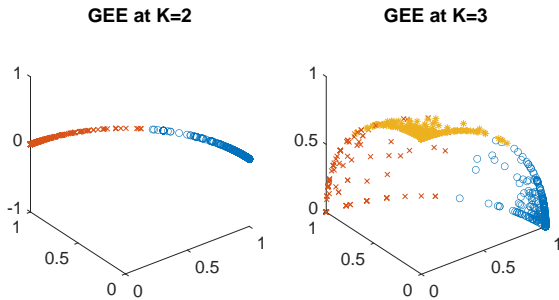


Fig. 4. Visualize the vertex embedding and community structure for the political blogs. Different colors represent different communities. The left panel is the vertex embedding using ground-truth size  $K = 2$ , while the right panel shows the ensemble embedding estimating 3 communities.

## 5 CONCLUSION

In this paper we proposed the graph encoder ensemble that simultaneously achieves graph embedding, community detection, and community size determination. It is easy to implement, computationally efficient, performs well against sparse graphs and unknown community size throughout the experiments. There are several interesting topics to

pursue for future works, such as a mathematical proof for the asymptotic clustering optimality under stochastic block model, further investigation into the theoretical and numerical properties of MRI, algorithm improvement for multi-level community detection, and applications to complicated network data such as dynamic and multi-modal graphs.

## REFERENCES

- [1] M. Girvan and M. E. J. Newman, "Community structure in social and biological networks," *Proceedings of National Academy of Science*, vol. 99, no. 12, pp. 7821–7826, 2002. 1
- [2] B. Karrer and M. E. J. Newman, "Stochastic blockmodels and community structure in networks," *Physical Review E*, vol. 83, p. 016107, 2011. 1
- [3] Y. Zhao, E. Levina, and J. Zhu, "Consistency of community detection in networks under degree-corrected stochastic block models," *Annals of Statistics*, vol. 40, no. 4, pp. 2266–2292, 2012. 1, 3
- [4] E. Abbe, "Community detection and stochastic block models: Recent developments," *Journal of Machine Learning Research*, vol. 18, no. 177, pp. 1–86, 2018. 1
- [5] K. Rohe, S. Chatterjee, and B. Yu, "Spectral clustering and the high-dimensional stochastic blockmodel," *Annals of Statistics*, vol. 39, no. 4, pp. 1878–1915, 2011. 1
- [6] D. Sussman, M. Tang, D. Fishkind, and C. Priebe, "A consistent adjacency spectral embedding for stochastic blockmodel graphs," *Journal of the American Statistical Association*, vol. 107, no. 499, pp. 1119–1128, 2012. 1
- [7] C. Gao, Z. Ma, A. Y. Zhang, and H. H. Zhou, "Community detection in degree-corrected block models," *Annals of Statistics*, vol. 46, no. 5, pp. 2153–2185, 2018. 1
- [8] V. D. Blondel, J. L. Guillaume, R. Lambiotte, and E. Lefebvre, "Fast unfolding of communities in large networks," *Journal of Statistical Mechanics: Theory and Experiment*, vol. 10008, p. 6, 2008. 1

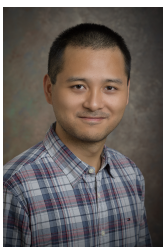
- [9] V. A. Traag, L. Waltman, and N. J. van Eck, "From louvain to leiden: guaranteeing well-connected communities," *Scientific Reports*, vol. 9, p. 5233, 2019. **1**
- [10] C. Shen, Q. Wang, and C. E. Priebe, "One-hot graph encoder embedding," *IEEE Transactions on Pattern Analysis and Machine Intelligence*, accepted, 2023. **1, 2**
- [11] R. Maclin and D. Opitz, "Popular ensemble methods: An empirical study," *Journal Of Artificial Intelligence Research*, vol. 11, pp. 169–198, 1999. **1**
- [12] L. Breiman, "Random forests," *Machine Learning*, vol. 4, no. 1, pp. 5–32, October 2001. **1**
- [13] S. P. Lloyd, "Least squares quantization in pcm," *IEEE Transactions on Information Theory*, vol. 28, no. 2, p. 129–137, 1982. **1**
- [14] E. W. Forgy, "Cluster analysis of multivariate data: efficiency versus interpretability of classifications," *Biometrics*, vol. 21, no. 3, p. 768–769, 1965. **1**
- [15] W. M. Rand, "Objective criteria for the evaluation of clustering methods," *Journal of the American Statistical Association*, vol. 66, no. 336, pp. 846–850, 1971. **1**
- [16] C. Priebe, Y. Parker, J. Vogelstein, J. Conroy, V. Lyzinskie, M. Tang, A. Athreya, J. Cape, and E. Bridgeford, "On a 'two truths' phenomenon in spectral graph clustering," *Proceedings of the National Academy of Sciences*, vol. 116, no. 13, pp. 5995–5600, 2019. **2**
- [17] P. J. Rousseeuw, "Silhouettes: a graphical aid to the interpretation and validation of cluster analysis," *Computational and Applied Mathematics*, vol. 20, pp. 53–65, 1987. **2**
- [18] D. L. Davies and D. W. Bouldin, "A cluster separation measure," *IEEE Transactions on Pattern Analysis and Machine Intelligence*, vol. 1, no. 2, pp. 224–227, 1989. **2**
- [19] P. Holland, K. Laskey, and S. Leinhardt, "Stochastic blockmodels: First steps," *Social Networks*, vol. 5, no. 2, pp. 109–137, 1983. **3**
- [20] T. Snijders and K. Nowicki, "Estimation and prediction for stochastic blockmodels for graphs with latent block structure," *Journal of Classification*, vol. 14, no. 1, pp. 75–100, 1997. **3**
- [21] R. A. Rossi and N. K. Ahmed, "The network data repository with interactive graph analytics and visualization," in *AAAI*, 2015. [Online]. Available: <https://networkrepository.com> **4**
- [22] H. Yin, A. R. Benson, J. Leskovec, and D. F. Gleich, "Local higher-order graph clustering," in *Proceedings of the 23rd ACM SIGKDD International Conference on Knowledge Discovery and Data Mining*, 2017, p. 555–564. **4**
- [23] L. Adamic and N. Glance, "The political blogosphere and the 2004 us election: Divided they blog," in *Proceedings of the 3rd International Workshop on Link Discovery*. New York: ACM Press, 2005, pp. 36–43. **4**



Youngser Park received the B.E. degree in electrical engineering from Inha University in Seoul, Korea in 1985, the M.S. and Ph.D. degrees in computer science from The George Washington University in 1991 and 2011 respectively. From 1998 to 2000 he worked at the Johns Hopkins Medical Institutes as a senior research engineer. From 2003 until 2011 he worked as a senior research analyst, and has been an associate research scientist since 2011 then research scientist since 2019 in the Center for Imaging Science at the Johns Hopkins University. At Johns Hopkins, he holds joint appointments in the The Institute for Computational Medicine and the Human Language Technology Center of Excellence. His current research interests are clustering algorithms, pattern classification, and data mining for high-dimensional and graph data.



Carey E. Priebe received the BS degree in mathematics from Purdue University in 1984, the MS degree in computer science from San Diego State University in 1988, and the PhD degree in information technology (computational statistics) from George Mason University in 1993. From 1985 to 1994 he worked as a mathematician and scientist in the US Navy research and development laboratory system. Since 1994 he has been a professor in the Department of Applied Mathematics and Statistics at Johns Hopkins University. His research interests include computational statistics, kernel and mixture estimates, statistical pattern recognition, model selection, and statistical inference for high-dimensional and graph data. He is a Senior Member of the IEEE, an Elected Member of the International Statistical Institute, a Fellow of the Institute of Mathematical Statistics, and a Fellow of the American Statistical Association.



Cencheng Shen received the BS degree in Quantitative Finance from National University of Singapore in 2010, and the PhD degree in Applied Mathematics and Statistics from Johns Hopkins University in 2015. He is assistant professor in the Department of Applied Economics and Statistics at University of Delaware. His research interests include graph inference, hypothesis testing, correlation and dependence.